BNL-111710-2016-JA

Blue emission of Eu^{2+}-doped transparent Alumina

Yan Yang[1], Lihua Zhang[2], Kim Kisslinger[2], Hua Wei[3], Charles L. Melcher[3], Yiquan Wu[1]*

[1]Kazuo Inamori School of Engineering, New York State College of Ceramics, Alfred University, Alfred, NY 14802, USA
[2]Center for Functional Nanomaterials, Brookhaven National Laboratory, Upton, New York, 11973-5000, USA
[3]Scintillation Materials Research Center, University of Tennessee, Knoxville, 37996, USA

*Email: wuy@alfred.edu

Abstract:

Blue light emissions from Eu^{2+}-doped transparent polycrystalline Al_2O_3 was observed at room temperature. The 0.1 at% Eu^{2+}-doped Al_2O_3 was fabricated by gelcasting and vacuum sintering method. The microstructure and the chemical composition of the vacuum-sintered Eu^{2+}-doped Al_2O_3 were characterized by Scanning Electric Microscopy (SEM), Transmittance Electron Microscopy (TEM), and Energy-dispersive X-ray spectroscopy (EDS). The phase composition was tested by X-Ray Diffraction pattern (XRD). The Photoluminescence of the Eu^{2+}-doped Al_2O_3were performed with excitation of UV light and showed the blue emission at 440nm. Radio-luminescence of Eu^{2+}-doped Al_2O_3 was also characterized by the illumination of X-ray and showed three mission bands at position 376nm, 575nm and 698nm.

Key words: Blue emission, Eu^{2+}-doped transparent Al_2O_3, Gelcasting, Vacuum sintering, photoluminescence, radio-luminescence

1. Introduction:

In radiation detection, inorganic scintillators play an important role in all medical diagnostic imaging modalities that use X-rays or gamma rays and many industrial measuring systems[1, 2]. The host matrix and emission center with high luminosity and fast response time are promising candidates. Recently the application of Ce^{3+} emission center with different matrix has attracted many researchers due to the parity and spin 5d-4f transition[3]. With increasing research in rear-earth element, Eu^{2+} with highly efficient and relative fast 5d-4f luminescence also draws the researchers' attention.

Optical transitions of divalent Europium ($4f^7$) Eu^{2+} ions have the potential applications for phosphors[4], lasers[5], or scintillator materials to detect ionizing radiation[6] for the reason of parity transition. High luminosity and fast decay time are mainly decided by the host matrix and emission center. Recently, various Eu^{2+} doped materials, such as SrI_2[7], $CsBa_2Br_5$[8], BaFI[9], Ba_2CsI_5[10], $LiCaAlF_6$ and $LiSrAlF_6$[11], with high output and acceptable scintillation decay time (faster than 1μs) have been achieved. However, for lack of chemical stability, applications of halide materials in scintillator are limited. Oxide ceramics, with the characters of high chemical stability, high transparency, and the feasibility of doping rare-earth

elements as induced luminescent centers, are ideal candidates for the new generation of scintillator materials. it reported the Ce-doped Garnet($Y_3Al_5O_{12}$) scintillator with superior scintillation properties[12, 13]. α-Al_2O_3 is a commonly-used optical host crystal and promising candidate for a new generation of emissive optical materials, which makes use of isolated impurities in ceramic matrices.

The Europium divalent ions could be obtained by reduction of Eu^{3+} to Eu^{2+} using laser induction[14], pulsed-laser deposition[15], chemical manipulation[16] or by annealing under a reducing atmosphere[17, 18]. Recently, some researchers found that Al is a key element to reduce Eu^{3+} to Eu^{2+}[13]. In the aspect of material processing, the blue emission center Eu^{2+} could be strongly affected by pressure. It has been observed that at low pressure (10^{-6} to 10^{-4} Mbar) range, the functional Eu^{2+}has been dominant among Eu^{2+} and Eu^{3+}[19].

In this study, Eu^{2+}-doped translucent Al_2O_3 was prepared by gelcasting and high-vacuum (10^{-6}~10^{-5}MBar) sintering with Eu_2O_3 as luminescent resource with photoluminescence blue emission at 440nm and radio luminescence at positions: 376nm, 575nm and 698nm.

2. Experiment:

Europium was introduced into Al_2O_3 in oxidized form Eu^{3+} (Eu_2O_3). High-purity α-Al_2O_3 powder (>99%) (CR-10, Baikowski, Annecy, France, D_{50} = 0.45μm), Eu_2O_3 (99.99%, Sigma, USA), de-ionized water and spontaneous gelling agent, behaving as dispersant at the same time, were mixed by ball-milling methods with solid loading of 38vol%. After de-gassing process, the resultant slurry was casted into mode for forming. After dried and pre-sintered in air, the green bodies were vacuumed sintered at 1800~1900°C for 5h.

Microstructures of Eu doped Al_2O_3 after vacuum sintering was characterized by SEM (FEI Quanta 200, USA) and TEM (JEOL2100F, Japan). Chemical composition was examined by BSE (FEI Quanta 200, USA) and EDS (JEOL2100F, Japan). Phase composition was tested by X-ray diffraction (XRD) (Bruker D2 Phaser, Germany) equipped with a Cu radiation (λ= 0.154 nm) in the range of 2θ=10~75°. Photoluminescence (PL) spectra were investigated by fluorescence spectrophotometer (JobinYvon Fluorolog-3spectrofluorometer, Horiba, USA) with Xenon lamp as the excitation source. Radio luminescence of Eu doped Al2O3 was performed under illumination of X-ray ().

3 Results and Discussion

3.1 Microstructure

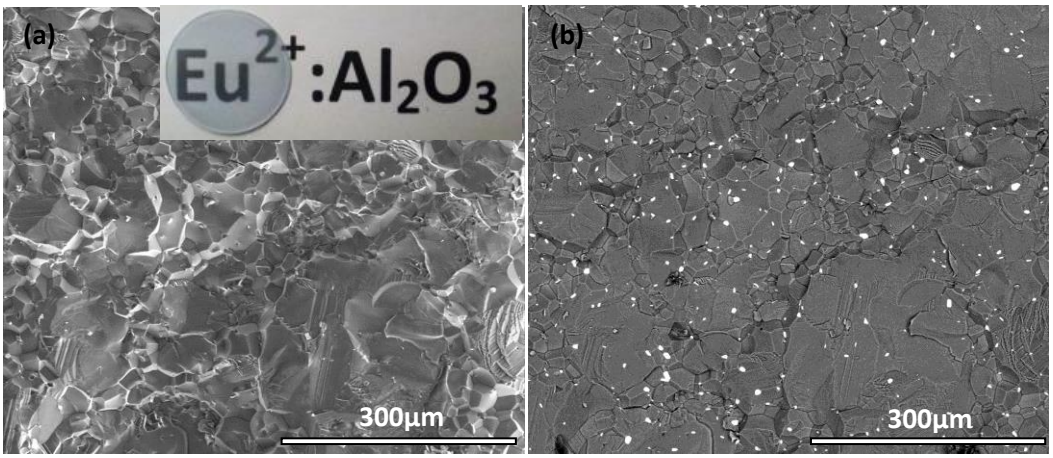

Fig. 1 0.1at% doped Al_2O_3 (a) SEM of cross-section; (b) BSE of the same area

Figure 1 shows the microstructure of 0.1 at% Eu^{2+}-doped Al_2O_3 after vacuum sintering. Figure 1(a) and (b) were recorded on the same area of the cross-section of vacuum sintered Al_2O_3. Only a few isolated pores were observed (Figure 1(a)), confirming that sample was close to the theoretical density. The grain size distributes in the range of 60~250μm, which is larger compared to pure translucent alumina with the grain size of 10~20μm[20]. The reason for this phenomenon may come from the fact that large size of the rare earth ions act as controlling factors on the grain growth speed, despite the very low Eu concentration. 0.1at% Eu^{2+} addition will increase the grain growth speed during sintering process. But there exists impurity phase on the microstructure of Eu^{2+}- doped Al_2O_3, shown in Fig. 1(b) (bright parts in BSE). The element composition was examined by EDS in Fig. 2. Obvious peaks for Eu were detected, denoting that the impurities are Eu-rich clusters. The segregation of Europium comes from un-dissolved Eu atoms, resulting from the large difference in ionic radius for Eu^{2+} (131pm) and Al^{3+} (67.5pm). Higher magnification of the cross-section was characterized by TEM in Fig. 3. It could see that the Eu-rich impurities entangle together with Al_2O_3 grains and grow along or through Al_2O_3 grain boundaries. Europium atoms tend to be segregated on the boundaries of Al_2O_3, in consistent with other results[21, 22].

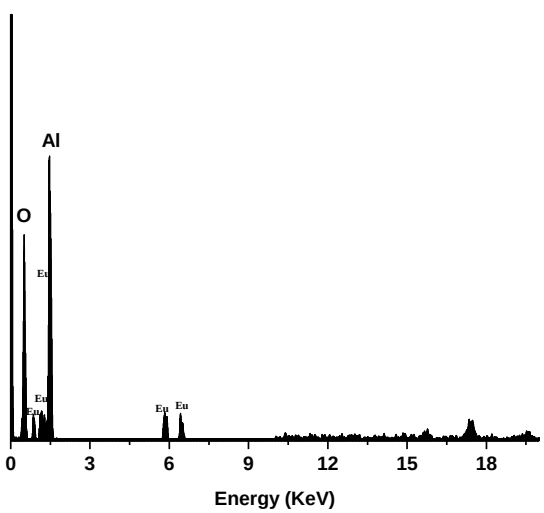

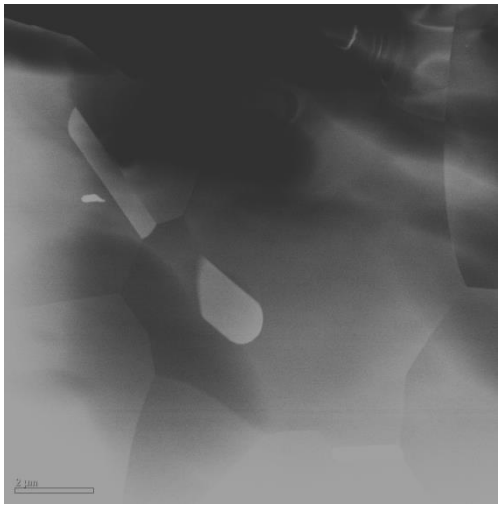

Fig. 2 EDS of 0.1at% Eu doped Al_2O_3 Fig.3 HAADF image of 0.1at% Eu doped Al_2O_3

3.2 Phase Identification

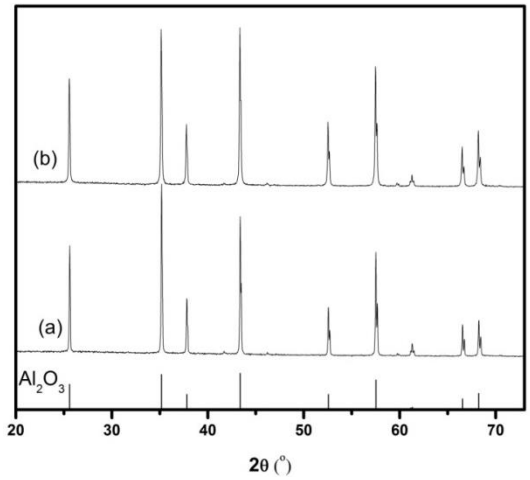

Fig. 4 XRD patterns of Al_2O_3 vacuum sintering (a) un-doped Al_2O_3, (b) 0.1at%Eu^{2+}-doped Al_2O_3

Phase constitution and lattice structure of translucent Al_2O_3 with and without Eu addition were examined by XRD patterns at 25°C, as shown in Fig. 4. The phase identification was analyzed by Diffrac EVA. The diffraction peak position of Eu-doped Al_2O_3 could be well indexed to un-doped Al_2O_3, in consistence with the standard trigonal α-Al_2O_3 (JCPDS # 00-042-1468) even though there exist impurities (Figure 1(b)), which could not be detected by XRD test. However, small shift of the diffraction peaks of Eu^{2+}-doped Al_2O_3 towards lower 2θ values was found compared with the un-doped Al_2O_3, coming from the expansion of the lattice parameters. The diffraction data was refined using Topas. The lattice parameters were calculated from the XRD patterns, summarized in Table 1. This result is in agreement with the analysis of the XRD data, which revealed significant increases in the lattice parameters a, c and cell volume when doped with Eu. This clearly indicates that the dopants are substituted into the lattice of the Al_2O_3.

Table 1 Comparison of lattice parameters before and after doping

Samples	Lattice parameters (Å)		Cell volume(Å^3)
	a	c	
Undoped Al_2O_3	4.757	12.989	254.602
0.1at%Eu doped Al_2O_3	4.761	13.000	255.202

3.3 Photoluminescence and Radio-luminescence Properties

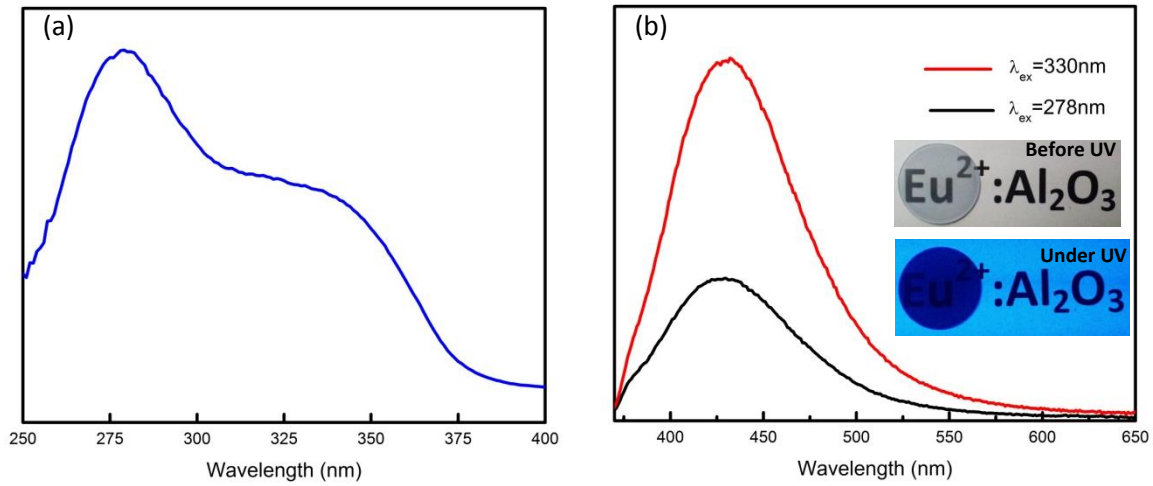

Fig. 5 Photoluminescence spectra of Eu^{2+}-doped Al_2O_3 (a) excitation spectrum monitored at 440nm; (b): emission spectra

Photoluminescence spectra were performed in Fig. 5. The UV excited luminescence of 0.1at% Eu^{2+}-doped Al_2O_3 was observed in the blue region with center at 440nm, in good agreement with the previous reports[23, 24]. The excitation spectrum(Fig.5(a)), monitoring at 440nm, shows two broad excitation bands, may coming from the split of the crystal field. This indicates that Eu^{2+} ions are located in low-symmetry sites with a broad crystal field distribution[25]. The emission spectrum at room temperature displays a broad band with a maximum at 440nm, leading to blue emission coming from the transition from $4f^6 5d^1$ to $4f^7$ ($^8S_{7/2}$). Even if there is large size relative to Al^{3+} and Eu^{2+}, the emission only takes place in the blue region, different from before report[19].

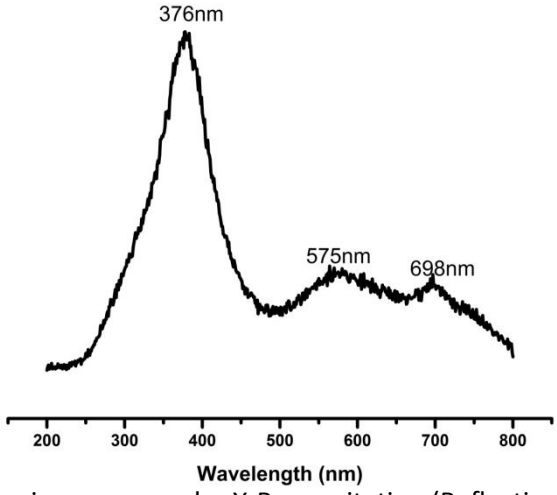

Fig. 6 Radio-luminescence under X-Ray excitation (Reflection mode)

Fig. 6 shows the radio luminescence properties of 0.10at% Eu^{2+}-Al_2O_3 under X-ray excitation (reflection mode), monitoring from 200n to 800nm at 1nm/step. It could be seen that there exist obvious emission

peaks with the position at 376nm, 575nm, 698nm. The maximum emission at 376nm is associated with $4f^6 5d$ $4f^7$ transition in Eu^{2+}, in consist with the report before[26]. The radio luminescence peak at 575nm and 698nm may coming from the defects of Al_2O_3 (Void of O^{2-}) during vacuum sintering process.

Conclusion:

Eu^{2+}-doped translucent polycrystalline Al_2O_3 were prepared by gelcasting and vacuum sintering methods with Eu_2O_3 as resource of Eu. With the presence of Al^{3+} and low oxygen partial pressure (10^{-6}Mba ~ 10^{-5} Mbar) during sintering process, only Eu^{2+} existed in the sintered translucent ceramic. The grain size of Eu^{2+}-doped Al_2O_3 after vacuum sintering is larger compared with pure polycrystalline Al_2O_3 with impurities appeared on the BES images. The phase is mainly trigonal α-Al_2O_3 with larger lattice parameters. Photoluminescence of blue light with center at 440nm was obtained by excitation at 278nm and 330nm ($4f^6 5d^1 \rightarrow 4f^7 (^8S_{7/2})$). Under X-ray excitation, the main emission peak sits at 376nm, which comes from d-f transition ($4f^6 5d \rightarrow 4f^7$).

ACKNOWLEDGMENTS: TEM experiments carried out at the Center for Functional Nanomaterials, Brookhaven National Laboratory, which is supported by the U.S. Department of Energy, Office of Basic Energy Sciences, under Contract No. DE-AC02-98CH10886.

References:

1. van Eijk, C.W., et al., *Ce< sup> 3+</sup> doped inorganic scintillators.* Nuclear Instruments and Methods in Physics Research Section A: Accelerators, Spectrometers, Detectors and Associated Equipment, 1994. **348**(2): p. 546-550.
2. Morton, E., et al., *Three-dimensional x-ray microtomography for medical and biological applications.* Physics in medicine and biology, 1990. **35**(7): p. 805.
3. Van Eijk, C.W., *Inorganic-scintillator development.* Nuclear Instruments and Methods in Physics Research Section A: Accelerators, Spectrometers, Detectors and Associated Equipment, 2001. **460**(1): p. 1-14.
4. Blasse, G. and A. Bril, *Fluorescence of Eu2+ activated alkaline-earth aluminates.* Philips Res. Rep, 1968. **23**: p. 201-206.
5. Bayer, E. and G. Schaack, *Two - Photon Absorption of CaF2: Eu2+.* physica status solidi (b), 1970. **41**(2): p. 827-835.
6. Alekhin, M.S., et al. *Scintillation properties and self absorption in SrI 2: Eu 2+*. in *Nuclear Science Symposium Conference Record (NSS/MIC), 2010 IEEE*. 2010. IEEE.
7. Cherepy, N., et al. *SrI2 scintillator for gamma ray spectroscopy*. in *SPIE Optical Engineering+ Applications*. 2009. International Society for Optics and Photonics.
8. Appleby, G., A. Edgar, and G. Williams, *Structure and photostimulated luminescent properties of Eu-doped< equation> M< sub> 2</sub>< font face='verdana'> Ba X< sub> 4</sub></equation>(< equation> M=< font face='verdana'> Cs</equation>, Rb;< equation> X=< font face='verdana'> Br</equation>, Cl).* Journal of applied physics, 2004. **96**(11): p. 6281-6285.

9. Gundiah, G., et al. *Scintillation properties of Eu 2+-activated barium fluoroiodide*. in *Nuclear Science Symposium Conference Record (NSS/MIC), 2009 IEEE*. 2009. IEEE.
10. Bourret-Courchesne, E., et al., *Eu< sup> 2+</sup>-doped Ba< sub> 2</sub> CsI< sub> 5</sub>, a new high-performance scintillator.* Nuclear Instruments and Methods in Physics Research Section A: Accelerators, Spectrometers, Detectors and Associated Equipment, 2009. **612**(1): p. 138-142.
11. Kirm, M., et al., *VUV spectroscopy of Eu doped LiCaAlF6 and LiSrAlF6 crystals.* physica status solidi (c), 2005. **2**(1): p. 418-421.
12. Wong, C., S. Rotman, and C. Warde, *Optical studies of cerium doped yttrium aluminum garnet single crystals.* Applied physics letters, 1984. **44**(11): p. 1038-1040.
13. Sugiyama, M., et al., *Basic study of Eu< sup> 2+</sup>-doped garnet ceramic scintillator produced by spark plasma sintering.* Optical Materials, 2012.
14. Lim, K.-S., et al., *Femtosecond laser-induced reduction in Eu-doped sodium borate glasses.* Journal of luminescence, 2007. **122**: p. 14-16.
15. Pillonnet, A., et al., *Valence state of europium doping ions during pulsed-laser deposition.* Journal of Physics D: Applied Physics, 2011. **44**(37): p. 375-402.
16. Biswas, A., C. Friend, and P. Prasad, *Spontaneous reduction of Eu< sup> 3+</sup> ion in Al co-doped sol–gel silica matrix during densification.* Materials Letters, 1999. **39**(4): p. 227-231.
17. Yang, C.-C., S.-Y. Chen, and D.-M. Liu, *Phase characterization and tunable photoluminescence of Eu-doped strontium-substituted nanohalophosphate.* Journal of crystal growth, 2006. **293**(1): p. 113-117.
18. Rakov, N. and G.S. Maciel, *Photoluminescence analysis of α-Al< sub> 2</sub> O< sub> 3</sub> powders doped with Eu< sup> 3+</sup> and Eu< sup> 2+</sup> ions.* Journal of Luminescence, 2007. **127**(2): p. 703-706.
19. Minardi, A., et al. *Divalent and Trivalent Europium Doped Alumina Waveguides Elaborated by Pulsed Laser Deposition*. in *MATERIALS RESEARCH SOCIETY SYMPOSIUM PROCEEDINGS*. 2001. Cambridge University Press.
20. Shimai, S., et al., *Spontaneous gelcasting of translucent alumina ceramics.* Optical Materials Express, 2013. **3**(8): p. 1000-1006.
21. Thompson, A.M., et al., *Dopant Distributions in Rare‐Earth‐Doped Alumina.* Journal of the American Ceramic Society, 1997. **80**(2): p. 373-376.
22. Yoshida, H., et al., *A change in the chemical bonding strength and high-temperature creep resistance in Al2O3 with lanthanoid oxide doping.* Philosophical Magazine A, 2002. **82**(3): p. 511-525.
23. Palilla, F.C., A.K. Levine, and M.R. Tomkus, *Fluorescent Properties of Alkaline Earth Aluminates of the Type MAl2 O 4 Activated by Divalent Europium.* Journal of the Electrochemical Society, 1968. **115**(6): p. 642-644.
24. Matsuzawa, T., et al., *A New Long Phosphorescent Phosphor with High Brightness, SrAl2 O 4: Eu2+, Dy3+.* Journal of The Electrochemical Society, 1996. **143**(8): p. 2670-2673.
25. Blasse, G., et al., *Fluorescence of Eu2+ activated silicates.* Philips Res. Rep, 1968. **23**: p. 189-200.
26. Shiran, N., et al., *Optical and scintillation properties of LiCaAlF< sub> 6</sub>: Eu crystal.* Journal of luminescence, 2003. **102**: p. 815-818.